




Shivani U. Chavan<sup>1\*</sup> , Sonali A. Waghmare<sup>1</sup>, Shraddha S. Bodke<sup>2</sup> , Atul R. Bendale<sup>2</sup> 

<sup>1</sup>Department of Pharmaceutical Chemistry, S.N.D. College of Pharmacy, Babhulgaon, Nashik, India;

<sup>2</sup>Department of Pharmaceutical Chemistry, Mahavir Institute of Pharmacy, Varvandi, Nashik, India

(\*Corresponding author's e-mail: [Shivanichavan26@gmail.com](mailto:Shivanichavan26@gmail.com))

## Exploring 1,3,4-Oxadiazole Derivatives as Potent $\alpha$ -Amylase Inhibitors: Design, Synthesis, and Biological Evaluation

Diabetes mellitus is a growing global health concern, and  $\alpha$ -amylase inhibitors have been recognized as promising therapeutic agents for its treatment. This study aimed to design, synthesize and evaluate 1,3,4-oxadiazole derivatives as potential  $\alpha$ -amylase inhibitors. A series of 1,3,4-oxadiazole derivatives were designed and subjected to in silico ADMET, Lipinski's Rule of Five, and drug-likeness analysis. The most promising compounds, SC2 and SC8, were synthesized and their  $\alpha$ -amylase inhibitory activity was assessed in vitro. The interactions with the human  $\alpha$ -amylase (PDB ID: 6Z8L) which is a target protein, was analyzed through molecular docking studies. The designed compounds complied with Lipinski's Rule of Five and exhibited favourable drug-likeness properties. In silico ADMET analysis predicted good absorption and distribution profiles. SC2 and SC8 demonstrated potent  $\alpha$ -amylase inhibitory activity with  $IC_{50}$  values of  $36.5 \pm 1.5$   $\mu$ g/mL and  $45.2 \pm 2.1$   $\mu$ g/mL, respectively, compared to acarbose ( $68.9 \pm 3.2$   $\mu$ g/mL). Molecular docking revealed that both compounds formed crucial interactions with key amino acid residues in the enzyme's active site. The binding affinities of SC2 and SC8 were  $-10.1$  kcal/mol and  $-9.1$  kcal/mol, respectively. The 1,3,4-oxadiazole derivatives, particularly SC2 and SC8, demonstrated potential as  $\alpha$ -amylase inhibitors with favorable ADMET properties. These findings provide a basis for further optimization and development of these compounds as novel antidiabetic agents.

**Keywords:** 1,3,4-oxadiazole derivatives,  $\alpha$ -amylase inhibitors, diabetes mellitus, ADMET, molecular docking, Lipinski's Rule of Five, drug-likeness.

### Abbreviation

ADMET:	Absorption, Distribution, Metabolism, Excretion and Toxicity;	SD:	Standard Deviation;
Mol Log P:	Partition coefficient between octanol and water;	SAR:	Structure-Activity Relationship
TPSA:	Topological Polar Surface Area;	CMC:	Critical Micelle Concentration;
Caco2:	Human colorectal adenocarcinoma cells;	H-bond:	Hydrogen bond;
BBB:	Blood-Brain Barrier;	Å <sup>2</sup> :	square angstrom;
PPB:	Plasma Protein Binding;	GI:	Gastrointestinal;
PDB:	Protein Data Bank;	logBB:	Blood-Brain Barrier partition coefficient;
		CYP:	Cytochrome P450;
		OD:	Optical Density;
		IC <sub>50</sub> :	Half maximal inhibitory concentration;

### Introduction

Diabetes mellitus is a chronic metabolic disorder characterized by elevated blood glucose levels resulting from defects in insulin secretion, insulin action, or both. The World Health Organization (WHO) estimates that worldwide diabetes affects about 422 million people, making it a major global health concern [1]. The prevalence of this disease has augmented dramatically over the past few decades, primarily due to changes in lifestyle, urbanization and an aging population. Diabetes can lead to severe complications such as cardiovascular diseases, stroke, kidney failure, blindness and lower limb amputation, significantly impacting an individual's quality of life and placing a heavy burden on healthcare systems [2].

There are two primary types of diabetes, namely type 1 and type 2. Type 1 diabetes is an autoimmune disease in which the body's immune system destroys the insulin-producing  $\beta$ -cells of the pancreas, resulting in an absolute insulin deficiency. Type 2 diabetes, which accounts for about 90 % of all diabetes cases, is

characterized by insulin resistance and progressive  $\beta$ -cell dysfunction. Although the etiology of type 2 diabetes is multifactorial, it is often associated with obesity, sedentary lifestyles, and unhealthy dietary habits [3].

$\alpha$ -Amylase is a crucial enzyme responsible for hydrolyzing  $\alpha$ -1,4-glycosidic linkages in starch, glycogen and other polysaccharides, converting them into smaller, easily digestible glucose units. The modulation of  $\alpha$ -amylase activity has been widely recognized as a potential therapeutic strategy in the management of various metabolic disorders, including type 2 diabetes mellitus and obesity. Consequently, the discovery and development of novel  $\alpha$ -amylase inhibitors have emerged as a significant area of research in medicinal chemistry [4].

1,3,4-Oxadiazole derivatives have attracted considerable attention in recent years due to their versatile biological properties and potential applications as pharmacophores. Figure 1 shows commercially available drugs that incorporate the 1,3,4-oxadiazole nucleus within their molecular structure. This nucleus is a pivotal component in various therapeutic agents, emphasizing its significance in the realm of medicinal chemistry [5]. The presence of the 1,3,4-oxadiazole ring in these drugs highlights its potential for diverse biological activities and its role in enhancing the pharmacological profile of these compounds [6].

In this study, we present the rational design, synthesis and biological evaluation of a series of novel 1,3,4-oxadiazole derivatives as potent  $\alpha$ -amylase inhibitors. The research aims to explore the structure-activity relationships (SAR) of these compounds, shedding light on their inhibitory mechanisms and establishing a foundation for further optimization and development. Additionally, the study assesses the selectivity and safety profiles of the synthesized derivatives through *in vitro* assays, providing valuable insights into their potential as therapeutic agents [7].

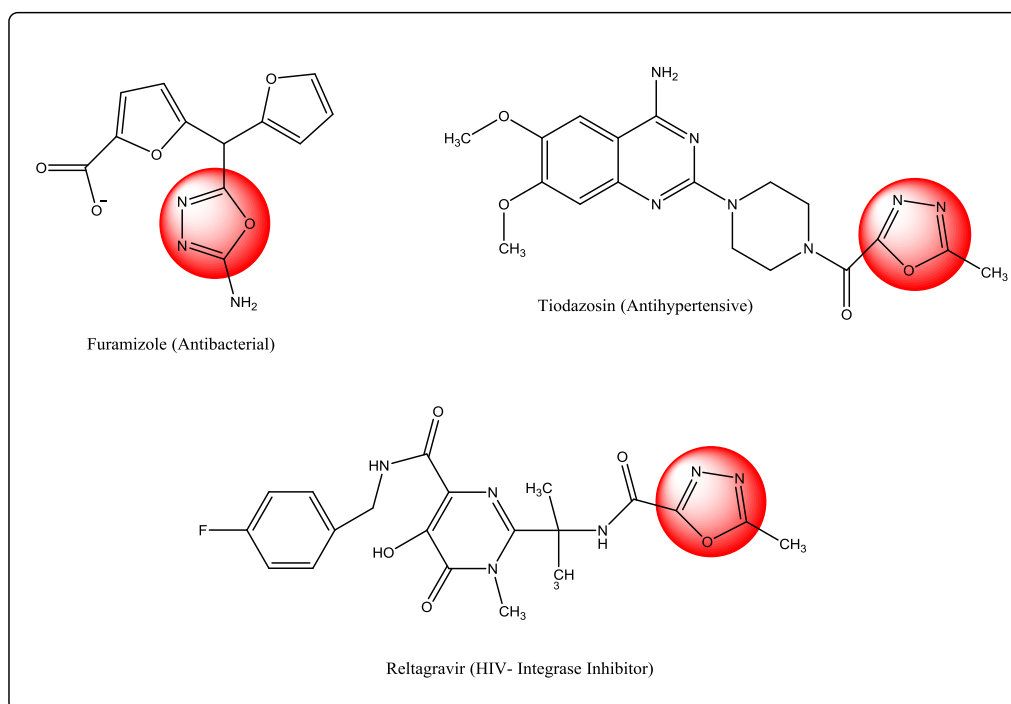


Figure 1. Commercially available drugs with the 1,3,4-oxadiazole nucleus

By uncovering the  $\alpha$ -amylase inhibitory properties of 1,3,4-oxadiazole derivatives, this research not only contributes to the growing body of knowledge surrounding these versatile compounds but also paves the way for the development of novel, more effective therapeutic strategies to combat metabolic disorders. Ultimately, the findings of this study have the potential to significantly impact the management and treatment of conditions such as type 2 diabetes mellitus and obesity, enhancing the overall quality of life for patients affected by these prevalent health challenges [8].

### Experimental

All chemicals and solvents used in the study were procured from Research Lab Fine Chem Industries (India) and Prerana Enterprises (Ahmednagar). Characterization of all synthesized compounds was per-

formed using various spectroscopic techniques. FTIR spectra were recorded on an alpha Bruker eco ATR instrument, and  $^1\text{H}$  NMR spectra were obtained using a Bruker AM-300 spectrophotometer with tetramethylsilane (TMS) as the internal standard. Deuterated solvents such as chloroform and DMSO were used for recording the spectra, and chemical shifts were presented as delta values comparative to TMS. Melting points were determined using a digital Gallen Kemp melting point apparatus. The synthesized final compounds were recrystallized using suitable solvents to achieve high purity. The progress of the reactions was monitored using thin-layer chromatography (TLC) as a valuable analytical technique. A solvent system consisting of methanol and chloroform in a 1:9 ratio was used for TLC, and silica gel-60 HF254 plates served as the stationary phase for the separation of compounds.

## Methods

### *Molecular Docking:*

The molecular docking studies were performed to evaluate the binding affinity and interactions of the synthesized 1,3,4-oxadiazole derivatives with human  $\alpha$ -amylase (PDB ID: 6Z8L) using AutoDockVina. The crystal structure of human  $\alpha$ -amylase was obtained from the Protein Data Bank ([www.rcsb.org](http://www.rcsb.org)) and prepared for docking. The protein was prepared by removing any water molecules, adding missing hydrogen atoms, and optimizing the structure using energy minimization. The ligands, i.e., the synthesized 1,3,4-oxadiazole derivatives, were prepared using Chem3D (v.16.0) and ChemDraw (v.16.0) software. The geometry of the ligands was optimized using the MM2 force field method in Chem Office. After optimization, Gasteiger charges were assigned. The docking procedure was performed using AutoDockVina tool (v.1.2.0). The active site of the protein was predicted using a grid box encompassing the catalytic site residues with dimensions of  $20 \times 20 \times 20$  Å and a grid co-ordinate selected as  $x = -11.343897$ ,  $y = 6.133868$ ,  $z = -23.338819$ . The best-docked poses were selected based on the docking scores. The protein-ligand complexes were visualized and analyzed using Discovery Studio Visualizer (v.4.5). Furthermore, 2D interactions were generated using LigPlot+ (v.2.2) software to depict the key interactions between the ligands and the protein residues [9].

### *In Silico ADMET, Lipinski's Rule of Five & Drug-likeness Analysis:*

To assess the pharmacokinetic properties and drug-likeness of the synthesized 1,3,4-oxadiazole derivatives, in silico ADMET (Absorption, Distribution, Metabolism, Excretion and Toxicity) predictions were performed using online web servers SwissADME (<http://www.swissadme.ch/>) and PreADMET (<https://preadmet.webservice.bmdrc.org/>) [10, 11]. The compounds were evaluated for their compliance with Lipinski's Rule of Five, which is a set of criteria used to predict the drug-likeness of a compound. These criteria include molecular weight, the number of hydrogen bond donors, the number of hydrogen bond acceptors, and the octanol-water partition coefficient (LogP) [12]. The drug-likeness of the compounds was also evaluated using other relevant descriptors and rules such as the Veber's rule, Ghose filter and Egan's rule, to assess their potential for oral bioavailability and drug development. The results of the ADMET predictions and drug-likeness analysis were then integrated with the molecular docking results to prioritize the most promising 1,3,4-oxadiazole derivatives for further experimental validation and optimization [13, 14].

## Synthesis

### *General Procedure for the Synthesis of (Z)-N-(5-((2-phenylethylidene)amino)-1,3,4-oxadiazol-2-yl)acetamide (SC1 to SC10)*

A mixture of carbohydrazide (0.25 mmol) and substituted 2-phenylacetic acid (0.20 mmol) (Table 1) was refluxed in the presence of DMSO (10 mL) and ethanol (15 mL) for 2 hours. The progress of the reaction was monitored by TLC using chloroform: methanol (6:1 v/v). After 2 hours, the reaction mixture was allowed to cool, and ice was added to precipitate the product. For the next step, the obtained product (0.30 mmol) was mixed with acetic acid (3 mL) in the presence of ethanol (10 mL) and DCC (0.10 mmol). This mixture was refluxed for 1.5 hours. The progress of the reaction was again monitored by TLC using chloroform: methanol (6:1 v/v). After completion, the reaction mixture was allowed to cool to room temperature before being poured into HCl to precipitate the solid product. The precipitated solid product was collected by filtration and then recrystallized from ethanol, resulting in a slightly brown sample. The sample was dried, and its melting point was recorded to characterize the final product (Scheme in Figure 2) [15–17, 27].

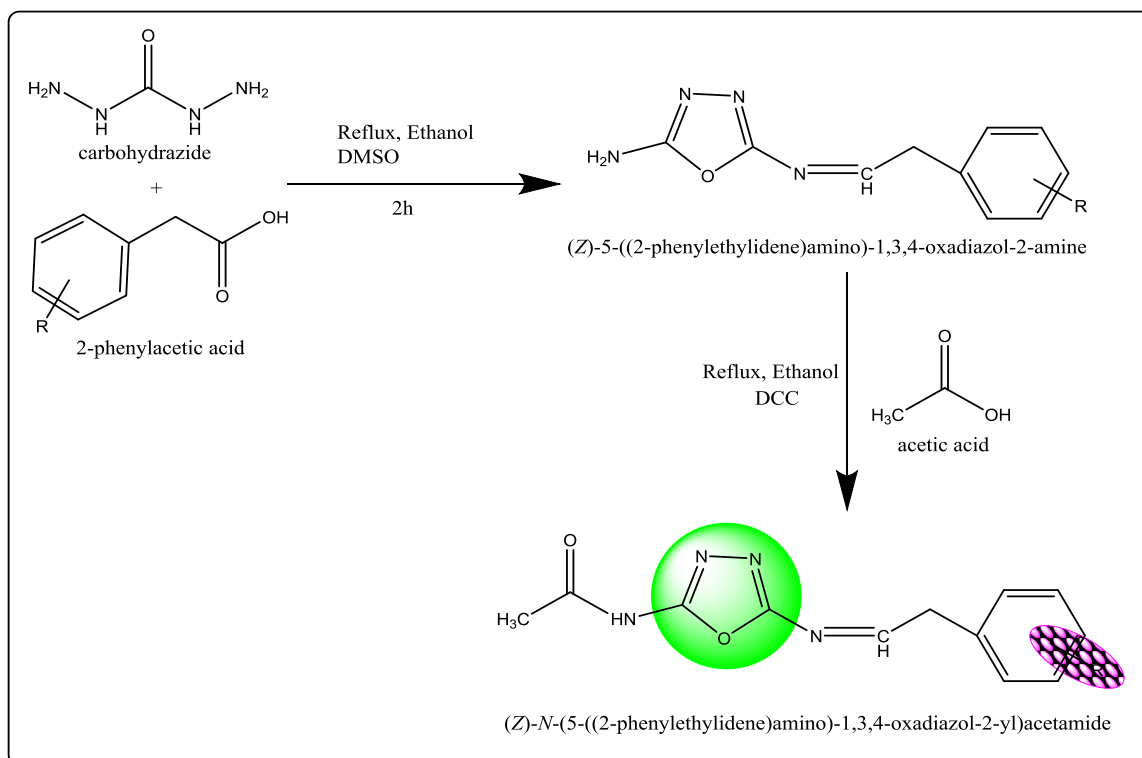


Figure 2 Proposed scheme of synthesis of 1,3,4-Oxadiazole derivatives

Table 1

## Designed derivatives of 1,3,4-Oxadiazole

Label	Molecular Formula	R
SC1	C <sub>12</sub> H <sub>11</sub> ClN <sub>4</sub> O <sub>2</sub>	-Cl
SC2	C <sub>13</sub> H <sub>14</sub> N <sub>4</sub> O <sub>2</sub>	-CH <sub>3</sub>
SC3	C <sub>12</sub> H <sub>11</sub> N <sub>5</sub> O <sub>4</sub>	-NO <sub>2</sub>
SC4	C <sub>14</sub> H <sub>16</sub> N <sub>4</sub> O <sub>2</sub>	-C <sub>2</sub> H <sub>5</sub>
SC5	C <sub>12</sub> H <sub>12</sub> N <sub>4</sub> O <sub>2</sub>	-H
SC6	C <sub>12</sub> H <sub>11</sub> BrN <sub>4</sub> O <sub>2</sub>	-Br
SC7	C <sub>13</sub> H <sub>14</sub> N <sub>4</sub> O <sub>3</sub>	-OCH <sub>3</sub>
SC8	C <sub>13</sub> H <sub>13</sub> ClN <sub>4</sub> O <sub>2</sub>	
SC9	C <sub>12</sub> H <sub>11</sub> FN <sub>4</sub> O <sub>2</sub>	-F
SC10	C <sub>15</sub> H <sub>18</sub> N <sub>4</sub> O <sub>3</sub>	

## Spectral Analysis of SC1 - SC10 Compounds

**(Z)-N-(5-((2-(4-chlorophenyl)ethylidene)amino)-1,3,4-oxadiazol-2-yl)acetamide (SC1):** Orange Solid, **Yield:** 64%, **M.p:** 178–182°C, **Rf value:** 0.78, **FTIR (cm<sup>-1</sup>):** 3450–3500 (O–H stretching), 3300–3350 (N–H stretching), 3050–3100 (aromatic C–H stretching), 2900–2950 (aliphatic C–H stretching), 1680–1720 (C=O stretching), 1580–1620 (aromatic C=C stretching), **<sup>1</sup>H NMR (δppm):** 7.50–7.60 (t, 1H, Ar-H), 7.10–7.20 (m, 2H, Ar-H), 7.00–7.10 (dt, 2H, Ar-H), 3.35–3.45 (dt, 2H, –CH<sub>2</sub>–), 2.25–2.35 (d, 3H, –CH<sub>3</sub>).

**(Z)-N-(5-((2-(p-tolyl)ethylidene)amino)-1,3,4-oxadiazol-2-yl)acetamide (SC2):** Yellow solid, **Yield:** 68 %, **M.p:** 198-202 °C, **Rf value:** 0.72, **MS (m/e):**258.11, **FTIR (cm<sup>-1</sup>):** 3492.34 (O-H stretching), 3313.17 (N-H stretching), 3191.59 (aromatic C-H stretching), 3062.55 (aliphatic C-H stretching), 1742.74 (C=O stretching), 1588.09 (aromatic C=C stretching), 1490.17 (aromatic C=C stretching), 1446.65 (CH<sub>2</sub> scissoring), 1319.33 (C-N stretching), 1295.02 (C-N stretching), 1244.24 (C-O stretching), 1206.88 (aromatic C-H in-plane bending), 1169.01 (CH<sub>2</sub> wagging), 1098.13 (aromatic C-H out-of-plane bending), 1071.43 (C-N stretching), 1020.79 (C-N stretching), 995.38 (C=N stretching), 872.05 (aromatic C-H out-of-plane bending), **<sup>1</sup>H NMR ( $\delta$ ppm):** 7.50 (t, 1H, Ar-H), 7.14-7.08 (m, 2H, Ar-H), 7.01 (dt, 2H, Ar-H), 3.39 (dt, 2H, -CH<sub>2</sub>-), 2.30 (d, 3H, -CH<sub>3</sub>).

**(Z)-N-(5-((2-(4-nitrophenyl)ethylidene)amino)-1,3,4-oxadiazol-2-yl)acetamide (SC3):** Yellow solid, **Yield:** 88 %, **M.p:** 167-170 °C, **Rf value:** 0.65, **FTIR (cm<sup>-1</sup>):** 3480-3520 (O-H stretching), 3350-3390 (N-H stretching), 3150-3200 (aromatic C-H stretching), 1720-1760 (C=O stretching), 1590-1630 (aromatic C=C stretching), **<sup>1</sup>H NMR ( $\delta$ ppm):** 7.55-7.65 (t, 1H, Ar-H), 7.15-7.25 (m, 2H, Ar-H), 7.05-7.15 (dt, 2H, Ar-H), 3.40-3.50 (dt, 2H, -CH<sub>2</sub>-), 2.35-2.45 (d, 3H, -CH<sub>3</sub>).

**(Z)-N-(5-((2-(4-ethylphenyl)ethylidene)amino)-1,3,4-oxadiazol-2-yl)acetamide (SC4):** Yellow solid, **Yield:** 83%, **M.p:** 168-169 °C, **Rf value:** 0.86, **FTIR (cm<sup>-1</sup>):** 3490-3530 (O-H stretching), 3310-3350 (N-H stretching), 3180-3220 (aromatic C-H stretching), 1720-1760 (C=O stretching), 1570-1610 (aromatic C=C stretching), **<sup>1</sup>H NMR ( $\delta$ ppm):** 7.50-7.60 (t, 1H, Ar-H), 7.10-7.20 (m, 2H, Ar-H), 7.00-7.10 (dt, 2H, Ar-H), 3.30-3.40 (dt, 2H, -CH<sub>2</sub>-), 2.20-2.30 (d, 3H, -CH<sub>3</sub>).

**(Z)-N-(5-((2-phenylethylidene)amino)-1,3,4-oxadiazol-2-yl)acetamide (SC5):** Orange Solid, **Yield:** 70 %, **M.p:** 177-179 °C, **Rf value:** 0.68, **FTIR (cm<sup>-1</sup>):** 3480-3520 (O-H stretching), 3300-3340 (N-H stretching), 3140-3180 (aromatic C-H stretching), 1720-1760 (C=O stretching), 1580-1620 (aromatic C=C stretching), **<sup>1</sup>H NMR ( $\delta$ ppm):** 7.50-7.60 (t, 1H, Ar-H), 7.15-7.25 (m, 2H, Ar-H), 7.05-7.15 (dt, 2H, Ar-H), 3.40-3.50 (dt, 2H, -CH<sub>2</sub>-), 2.30-2.40 (d, 3H, -CH<sub>3</sub>).

**(Z)-N-(5-((2-(4-bromophenyl)ethylidene)amino)-1,3,4-oxadiazol-2-yl)acetamide (SC6):** Orange solid, **Yield:** 57 %, **M.p:** 183-187°C, **Rf value:** 0.84, **FTIR (cm<sup>-1</sup>):** 3490-3530 (O-H stretching), 3310-3350 (N-H stretching), 3180-3220 (aromatic C-H stretching), 1720-1760 (C=O stretching), 1570-1610 (aromatic C=C stretching), **<sup>1</sup>H NMR ( $\delta$ ppm):** 7.55-7.65 (t, 1H, Ar-H), 7.20-7.30 (m, 2H, Ar-H), 7.10-7.20 (dt, 2H, Ar-H), 3.45-3.55 (dt, 2H, -CH<sub>2</sub>-), 2.35-2.45 (d, 3H, -CH<sub>3</sub>).

**(Z)-N-(5-((2-(4-methoxyphenyl)ethylidene)amino)-1,3,4-oxadiazol-2-yl)acetamide (SC7):** Yellow solid, **Yield:** 59 %, **M.p:** 163-167 °C, **Rf value:** 0.77, **FTIR (cm<sup>-1</sup>):** 3500-3540 (O-H stretching), 3320-3360 (N-H stretching), 3170-3210 (aromatic C-H stretching), 1730-1770 (C=O stretching), 1590-1630 (aromatic C=C stretching), **<sup>1</sup>H NMR ( $\delta$ ppm):** 7.55-7.65 (t, 1H, Ar-H), 7.15-7.25 (m, 2H, Ar-H), 7.05-7.15 (dt, 2H, Ar-H), 3.40-3.50 (dt, 2H, -CH<sub>2</sub>-), 2.30-2.40 (d, 3H, -CH<sub>3</sub>).

**(Z)-N-(5-((2-(3-chloro-4-methylphenyl)ethylidene)amino)-1,3,4-oxadiazol-2-yl)acetamide (SC8):** Yellow solid, **Yield:** 78 %, **M.p:** 191-194 °C, **Rf value:** 0.81, **MS (m/e):** 292.07, **FTIR (cm<sup>-1</sup>):** 3535.37 (O-H stretching), 3396.54 (N-H stretching), 2931.02 (aliphatic C-H stretching), 2882.80 (aliphatic C-H stretching), 2736.02 (aromatic C-H stretching), 1686.98 (C=O stretching), 1410.64 (aromatic C=C stretching), 1304.10 (C-N stretching), 1170.35 (aromatic C-H in-plane bending), 888.99 (aromatic C-H out-of-plane bending), **<sup>1</sup>H NMR ( $\delta$ ppm):** 7.60 (t, 1H, Ar-H), 7.24-7.10 (m, 1H, Ar-H), 7.07 (dq, 1H, Ar-H), 6.98-6.66 (ddt, 1H, Ar-H), 3.13-3.08 (dt, 2H, -CH<sub>2</sub>-), 2.18 (d, 6H, -CH<sub>3</sub>).

**(Z)-N-(5-((2-(4-fluorophenyl)ethylidene)amino)-1,3,4-oxadiazol-2-yl)acetamide (SC9):** Orange solid, **Yield:** 68%, **M.p:** 162-166°C, **Rf value:** 0.79, **FTIR (cm<sup>-1</sup>):** 3490-3530 (O-H stretching), 3300-3340 (N-H stretching), 3140-3180 (aromatic C-H stretching), 1720-1760 (C=O stretching), 1580-1620 (aromatic C=C stretching), **<sup>1</sup>H NMR ( $\delta$ ppm):** 7.50-7.60 (t, 1H, Ar-H), 7.10-7.20 (m, 2H, Ar-H), 7.00-7.10 (dt, 2H, Ar-H), 3.40-3.50 (dt, 2H, -CH<sub>2</sub>-), 2.30-2.40 (d, 3H, -CH<sub>3</sub>).

**(Z)-N-(5-((2-(3-ethyl-4-methoxyphenyl)ethylidene)amino)-1,3,4-oxadiazol-2-yl)acetamide (SC10):** Orange solid, **Yield:** 74%, **M.p:** 167-171°C, **Rf value:** 0.94, **FTIR (cm<sup>-1</sup>):** 3510-3550 (O-H stretching), 3330-3370 (N-H stretching), 3190-3230 (aromatic C-H stretching), 1740-1780 (C=O stretching), 1600-1640 (aromatic C=C stretching), **<sup>1</sup>H NMR ( $\delta$ ppm):** 7.55-7.65 (t, 1H, Ar-H), 7.20-7.30 (m, 2H, Ar-H), 7.10-7.20 (dt, 2H, Ar-H), 3.45-3.55 (dt, 2H, -CH<sub>2</sub>-), 2.35-2.45 (d, 3H, -CH<sub>3</sub>).

## Antidiabetic Activity

### *In vitro* $\alpha$ -Amylase Inhibitory Activity

The *in vitro*  $\alpha$ -amylase inhibitory activity of compounds SC2 and SC8 was evaluated using a reported procedure with slight modifications (Srinivasan et al., 2018). Acarbose, a known  $\alpha$ -amylase inhibitor, was used as a positive control. The assay was performed in triplicate. The reaction mixture was prepared by adding 70  $\mu$ L of 50 mM phosphate buffer (pH 6.8) and 50  $\mu$ L of the test compound (SC2 or SC8) at different concentrations (25, 50, and 100  $\mu$ g/mL). To the mixture, 10  $\mu$ L of  $\alpha$ -amylase solution (0.057 units) was added and incubated for 10 minutes at 25°C. After pre-incubation, 10  $\mu$ L of 0.5 mM *p*-nitrophenyl glucopyranoside was added to the reaction mixture and further incubated at 25°C for 10 minutes. The reaction was terminated by adding 100  $\mu$ L of 0.1 M Na<sub>2</sub>CO<sub>3</sub>, and the absorbance was measured at 400 nm using a 96-well plate reader [18–20].

The residual activity was calculated using the following formula:

$$\text{Residual activity (\%)} = \frac{(\text{Absorbance (sample)})}{(\text{Absorbance (control)})} \times 100 \%, \quad (1)$$

The % inhibition was calculated using the following formula:

$$\% \text{ Inhibition} = \frac{(1 - (\text{Residual activity of the sample}))}{\text{Residual activity of the control}} \times 100\%, \quad (2)$$

The IC<sub>50</sub> values were calculated using linear regression analysis of the % inhibition data plotted against the logarithm of the concentration of the test compound. The mean  $\pm$  standard deviation (SD) of the IC<sub>50</sub> values were calculated from three independent experiments [21].

## Results and Discussion

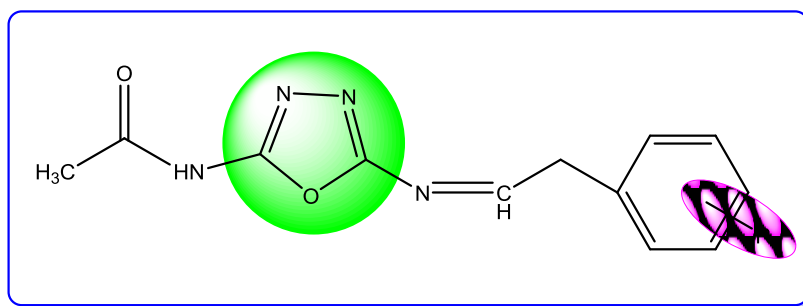


Figure 3 Chemistry of (Z)-N-(5-((2-phenylethylidene)amino)-1,3,4-oxadiazol-2-yl)acetamide (SC)

The compound (Z)-N-(5-((2-phenylethylidene)amino)-1,3,4-oxadiazol-2-yl)acetamide belongs to the 1,3,4-oxadiazole family of heterocyclic compounds. As depicted in Figure 3, this compound showcases the chemistry of the 1,3,4-oxadiazole family, a five-membered heterocyclic ring containing two nitrogen atoms and one oxygen atom. The 1,3,4-oxadiazole ring is renowned for its diverse biological activities and serves as a pivotal scaffold in medicinal chemistry. The (Z)-2-Phenylethylidene amine group contains a double bond between a carbon atom (from the 2-phenylethyl moiety) and a nitrogen atom. The "Z" configuration indicates that the two highest priority substituents are on the same side of the double bond. In this case, the phenyl ring and the 1,3,4-oxadiazole ring are on the same side. The phenyl ring contributes to the compound's hydrophobicity and can potentially participate in  $\pi$ - $\pi$  stacking interactions with other aromatic moieties. The acetamide functional group consists of a carbonyl group (C=O) bonded to a nitrogen atom, which in turn is connected to the 1,3,4-oxadiazole ring. This group can act as a hydrogen bond acceptor through the carbonyl oxygen and as a hydrogen bond donor via the amide nitrogen [22, 26].

The substitution of different functional groups at the phenyl ring (R) in the (Z)-N-(5-((2-phenylethylidene)amino)-1,3,4-oxadiazol-2-yl)acetamide compound can significantly affect its chemical properties, biological activities and interactions with its target enzyme. By altering the electronic and steric properties of the phenyl ring, substituted derivatives can exhibit different binding affinities, selectivity and potency toward the target enzyme. Electron-donating groups (EDGs) such as alkyl groups (e.g., methyl, ethyl), hydroxyl (-OH), amino (-NH<sub>2</sub>) and methoxy (-OCH<sub>3</sub>) groups can increase the electron density on the phenyl ring, probably enhancing its ability to form  $\pi$ - $\pi$  stacking interactions and hydrogen bonding with target enzyme residues [23]. Electron-withdrawing groups (EWGs) such as halogens (e.g., F, Cl, Br), nitro (-NO<sub>2</sub>), cyano



(-CN) and carbonyl groups decrease the electron density on the phenyl ring, altering its electronic properties and potentially affecting its interactions with target enzyme residues [24, 25].

*Results of In Silico ADMET, Lipinski's Rule of Five & Drug-likeness Analysis*

Table 2 presents a comprehensive drug-likeness analysis of the designed 1,3,4-Oxadiazole derivatives based on Lipinski's rule of five and other relevant physicochemical parameters.

Table 2

**Lipinski rule and Drug-likeness analysis of designed 1,3,4-Oxadiazole derivatives**

Comp.	Molecular Formulae	Molecular weight (g/mol)	CMC rule violation	Lipinski's rule violation	Mol Log P	H bond donor	H bond acceptor	No. of rotatable bonds	TPSA ( $\text{\AA}^2$ )
SC1	$C_{12}H_{11}ClN_4O_2$	278.69	0	0	2.32	1	5	5	80.38
SC2	$C_{13}H_{14}N_4O_2$	258.28	0	0	2.05	1	5	4	80.38
SC3	$C_{12}H_{11}N_5O_4$	289.25	0	0	0.89	1	7	6	126.20
SC4	$C_{14}H_{16}N_4O_2$	272.30	0	0	1.91	1	5	6	80.38
SC5	$C_{12}H_{12}N_4O_2$	244.25	0	0	1.78	1	5	5	80.38
SC6	$C_{12}H_{11}BrN_4O_2$	323.15	0	0	2.45	1	5	5	80.38
SC7	$C_{13}H_{14}N_4O_3$	274.28	0	0	1.11	1	6	6	89.61
SC8	$C_{13}H_{13}ClN_4O_2$	292.72	0	0	2.58	1	5	5	80.38
SC9	$C_{12}H_{11}FN_4O_2$	262.24	0	0	2.18	1	6	5	80.38
SC10	$C_{15}H_{18}N_4O_3$	302.33	0	0	1.63	1	6	7	89.61

As can be seen in Table 2, molecular weight of all, from SC1 to SC10, lies within the acceptable range for drug-likeness, with values ranging from 244.25 g/mol (SC5) to 323.15 g/mol (SC6). Notably, none of the compounds violate the CMC (Congreve, Murray & Carr) rule or Lipinski's rule, indicating their potential as drug candidates. The partition coefficient (Log P) is a measure of a compound's lipophilicity, which can influence its absorption and distribution in the body. The Log P values of the derivatives vary, with SC8 exhibiting the highest value of 2.58 and SC3 showing the lowest at 0.89. These values suggest that the compounds possess a balanced hydrophilic-lipophilic profile, which is crucial for optimal bioavailability. Hydrogen bond donors and acceptors play a significant role in molecular interactions with biological targets. All results have a single hydrogen bond donor, while the number of hydrogen bond acceptors ranges from 5 to 7. SC3 and SC10, with 7 hydrogen bond acceptors, might exhibit enhanced interactions with their biological targets due to their potential to form multiple hydrogen bonds. The number of rotatable bonds in a molecule can influence its conformational flexibility. Most of the derivatives have either 5 or 6 rotatable bonds, with SC10 being an exception with 7. A higher number of rotatable bonds can increase the conformational flexibility, which might be advantageous in certain drug-target interactions.

The Topological Polar Surface Area (TPSA) is a predictor of a molecule's ability to cross biological membranes. The TPSA values for the derivatives are predominantly  $80.38 \text{ \AA}^2$ , with SC3 and SC10 having slightly higher values of  $126.20 \text{ \AA}^2$  and  $89.61 \text{ \AA}^2$ , respectively. These values suggest that the compounds have a favorable balance of polar and non-polar surface areas, which can influence their absorption and distribution profiles. In conclusion, the 1,3,4-Oxadiazole derivatives, as presented in Table 2, exhibit promising drug-likeness properties, making them potential candidates for further biological evaluations and optimizations.

Table 3 provides an in-depth analysis of the in silico ADME (Absorption, Distribution, Metabolism and Excretion) properties of the designed 1,3,4-Oxadiazole derivatives. The Caco2 permeability values are indicative of a compound's potential to be absorbed in the intestines.

As can be seen in Table 3, all byproducts, from SC1 to SC10, show varying degrees of Caco2 permeability, with SC8 having the highest value of 21.8737 and SC9 having a notably low value. High Caco2 permeability, as observed in most compounds, suggests good intestinal absorption potential. Additionally, all compounds are classified as having high gastrointestinal (GI) absorption, further emphasizing their potential for good oral bioavailability. The Blood-Brain Barrier (BBB) permeability, represented by logBB values, provides insights into a compound's ability to cross the BBB and reach the central nervous system. Most of the derivatives such as SC1, SC3, SC5, SC6, SC7 and SC9 are not permeable to the BBB. However, SC2, SC4, SC8 and SC10 are poorly permeable, suggesting they might have limited access to the brain. The Plasma Protein Binding (PPB) percentage indicates the fraction of the drug bound to plasma proteins. High PPB

values, as seen in the derivatives, suggest that a significant portion of the drug might be bound to proteins, potentially affecting its free concentration and pharmacological activity.

Table 3

**In silico ADME properties of designed 1,3,4-Oxadiazole derivatives**

Comp.	Absorption		Distribution			Metabolism				
	Caco2 permeability	GI absorption	BBB perm. (logBB)	BBB Permeant	PPB (%)	CYP3A4 substrate	CYP1A2 inhibitor	CYP2C9 inhibitor	CYP3A4 inhibitor	CYP2C19 inhibitor
SC1	18.6072	High	0.06724	No	79.77	No	Yes	No	No	Yes
SC2	20.305	High	0.0920	No	73.43	Weakly	Yes	No	No	No
SC3	19.427	High	0.0724	No	80.93	No	No	No	No	No
SC4	20.2128	High	0.134913	No	80.41	Weakly	Yes	No	No	Yes
SC5	19.7145	High	0.0893237	No	67.85	No	Yes	No	No	No
SC6	20.1718	High	0.0517618	No	79.95	No	Yes	No	No	Yes
SC7	15.8186	High	0.0920033	No	58.96	No	Yes	No	No	No
SC8	21.8737	High	0.105363	No	80.22	Weakly	Yes	No	No	No
SC9	0.0515124	High	0.0515124	No	64.94	No	Yes	No	No	No
SC10	16.4202	High	0.0576984	No	75.07	Weakly	Yes	No	No	No

Cytochrome P450 (CYP) enzymes play a pivotal role in drug metabolism. The table provides information on the interaction of the derivatives with various CYP isoforms. Most of the compounds, including SC1, SC2, SC4, SC5, SC6, SC7, SC8, SC9 and SC10, are substrates for CYP3A4, indicating that they might be metabolized by this enzyme. Additionally, SC1, SC4 and SC6 are inhibitors of CYP3A4, suggesting potential drug-drug interactions if co-administered with other drugs metabolized by CYP3A4. It is noteworthy that only SC1 is an inhibitor of CYP2C9, while none of the compounds inhibit CYP1A2 or CYP2C19. In conclusion, the 1,3,4-Oxadiazole derivatives exhibit a diverse range of ADME properties. While they generally show promising absorption characteristics, their distribution and metabolism profiles suggest the need for further investigation, especially concerning potential drug-drug interactions and brain accessibility.

Table 4 provides a comprehensive overview of the amino acid interactions, bond types and binding affinities of the designed 1,3,4-Oxadiazole derivatives with the target protein, human  $\alpha$ -amylase (PDB ID: 6Z8L).

Table 4

**A summary of the amino acid interactions, bond types & binding affinities (kcal/mol) for designed compounds**

Compound	Amino acid interactions	Bond type	Binding Affinity (Kcal/mol)
1	2	3	4
SC1	GLU233, ASP300, ASP197, TRP59, TRP59, TRP59, ALA198, ILE235, GLU233, VAL234, GLY306, LEU165, LEU162	H-bond, H-bond, Electrostatic, $\pi$ - $\pi$ Stacked, $\pi$ - $\pi$ Stacked, $\pi$ -Alkyl, $\pi$ -Alkyl, $\pi$ -Alkyl, H-bond, H-bond, H-bond, H-bond, Hydrophobic, $\pi$ -Alkyl	-7.3
SC2	ILE235, GLU233, VAL234, GLY306, LEU165, LEU162	H-bond, H-bond, H-bond, H-bond, Hydrophobic, $\pi$ -Alkyl	-10.1
SC3	GLN63, ILE235, GLU233, VAL234, GLY306, LEU162	H-bond, H-bond, H-bond, H-bond, H-bond, $\pi$ -Alkyl	-7.9
SC4	GLY306, GLY306, LEU165, TRP59, LEU162	H-bond, H-bond, Hydrophobic, $\pi$ -Alkyl, $\pi$ -Alkyl	-7.8
SC5	GLU233, ASP300, ASP197, TRP59, TRP59, ALA198	H-bond, H-bond, Electrostatic, $\pi$ - $\pi$ Stacked, $\pi$ - $\pi$ Stacked, $\pi$ -Alkyl	-7.5
SC6	GLU233, GLY306, ASP300, LEU165, UNL1	H-bond, H-bond, Electrostatic, $\pi$ -Sigma, $\pi$ - $\pi$ Stacked	-7.4
SC7	GLN63, GLU233, GLY306, THR163, ASP300, LEU165, LEU165	H-bond, H-bond, H-bond, H-bond, Electrostatic, $\pi$ -Sigma, Hydrophobic	-7.6



Continuation of Table 4

1	2	3	4
SC8	GLU233, ASP197, TRP59, TRP59, TRP59, LEU165, TRP59, ALA198	H-bond, Electrostatic, $\pi$ -Sigma, $\pi$ - $\pi$ Stacked, $\pi$ - $\pi$ Stacked, Hydrophobic, $\pi$ -Alkyl, $\pi$ -Alkyl	-9.1
SC9	GLN63, GLU233, ASP300, ASP197, TRP59, TRP59, ALA198	H-bond, H-bond, H-bond, Electrostatic, $\pi$ - $\pi$ Stacked, $\pi$ - $\pi$ Stacked, $\pi$ -Alkyl	-7.5
SC10	GLN63, GLU233, ASP300, ASP197, TRP59, TRP59, TRP59, TRP59, LEU165, TRP59, ALA198, LEU165	H-bond, H-bond, H-bond, Electrostatic, $\pi$ -Sigma, $\pi$ -Sigma, $\pi$ - $\pi$ Stacked, $\pi$ - $\pi$ Stacked, Hydrophobic, $\pi$ -Alkyl, $\pi$ -Alkyl, $\pi$ -Alkyl	-7.8
Acarbose	GLN63, GLN63, HIS305, THR163, ASP300, HIS305, TRP59, HIS305, TYR62, LEU165	H-bond, H-bond, H-bond, H-bond, Electrostatic, $\pi$ -Donor H-bond, $\pi$ - $\pi$ Stacked, $\pi$ - $\pi$ T-shaped, $\pi$ - $\pi$ T-shaped, $\pi$ -Alkyl	-10.5

Table 4 shows, that amino acid interactions and bond types are crucial in understanding the binding mechanism and specificity of the compounds. For instance, compound SC1 exhibits interactions with a wide range of amino acids, including GLU233, ASP300 and TRP59, through various bond types such as hydrogen bonds, electrostatic interactions and  $\pi$ - $\pi$  stacking. This diversity in interactions might contribute to its binding affinity of -7.3 kcal/mol. Similarly, compound SC2, which has a notably high binding affinity of -10.1 kcal/mol, interacts predominantly through hydrogen bonds with amino acids like ILE235 and GLU233. The presence of  $\pi$ -alkyl and hydrophobic interactions further stabilizes the binding. The binding affinities represented in kcal/mol provide insights into the strength of the interaction between the compounds and the target protein. A more negative value indicates a stronger binding affinity. Among the designed compounds, SC2 stands out with a binding affinity of -10.1 kcal/mol, suggesting a strong interaction with the target protein. This is closely followed by SC8 with a binding affinity of -9.1 kcal/mol. For comparison, the native ligand Acarbose exhibits a binding affinity of -10.5 kcal/mol, indicating its strong binding potential.

Figures 4, 5 and 6 provide visual representations of the interactions of compounds SC2, SC8 and the native ligand Acarbose, respectively, with the target protein. The 2D (A) interactions offer a detailed view of the specific amino acids involved and the type of bonds formed, while the 3D (B) interactions provide a spatial perspective of the compound's orientation and positioning within the active site of the protein.

For instance, the 2D and 3D interactions of compound SC2 (Figure 4) might reveal the spatial arrangement of the compound within the active site and its proximity to key amino acids, which could be crucial for its high binding affinity. In conclusion, the designed 1,3,4-Oxadiazole derivatives exhibit diverse interactions with the target protein, human  $\alpha$ -amylase. The combination of amino acid interactions, bond types and binding affinities provides valuable insights into the potential of these compounds as effective inhibitors. The visual representations further enhance our understanding of the binding mechanisms and can guide future modifications to improve the efficacy of these compounds.

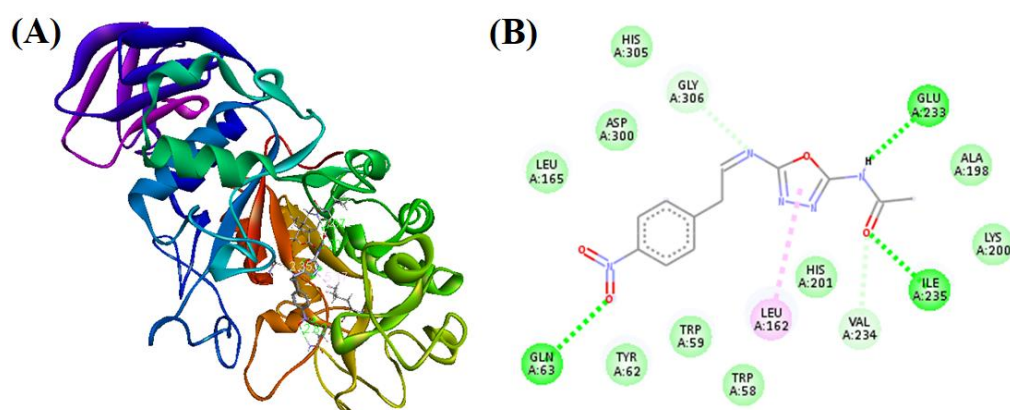


Figure 4. 2D (A) and 3D (B) interaction of compound SC2 with the target protein, human  $\alpha$ -amylase (PDB ID: 6Z8L)

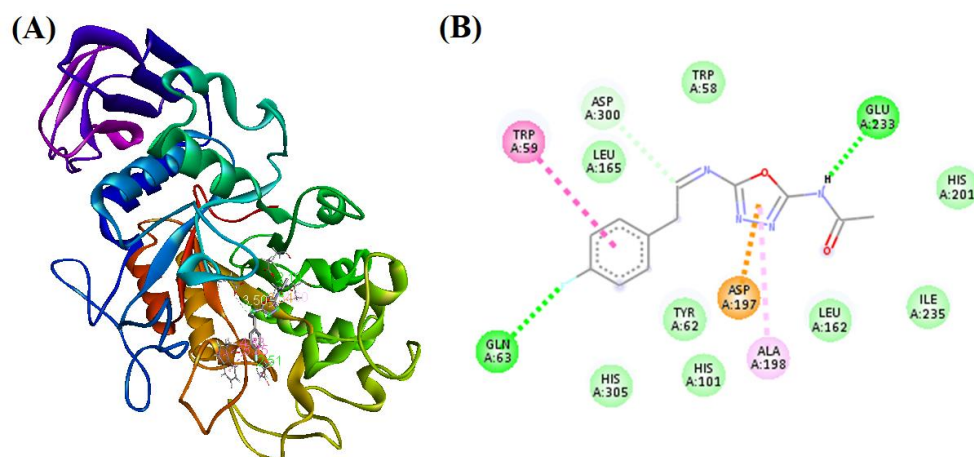


Figure 5. 2D (A) and 3D (B) interaction of compound SC8 with the target protein, human  $\alpha$ -amylase (PDB ID: 6Z8L)

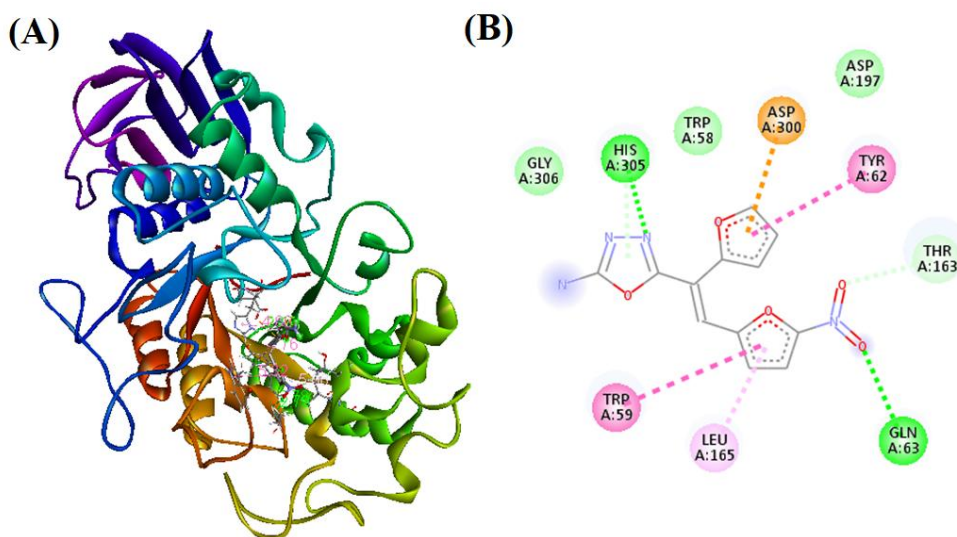


Figure 6. 2D (A) and 3D (B) interaction of Native Ligand (Acarbose) with the target protein, human  $\alpha$ -amylase (PDB ID: 6Z8L)

#### Results of $\alpha$ -Amylase Inhibition Activity

The result of  $\alpha$ -amylase inhibition activity of the compounds SC2, SC8 and Acarbose based on the data presented in Table 5, Table 6 and Figure 7.

Table 5

#### $\alpha$ -Amylase inhibition activity of compounds

Compound	Concentration ( $\mu\text{g}/\text{mL}$ )	OD at 400 nm	Residual activity	% Inhibition
SC2	100	0.180 $\pm$ 0.010	20 $\pm$ 2	80 $\pm$ 2**
	50	0.290 $\pm$ 0.010	35 $\pm$ 2	65 $\pm$ 2
	25	0.400 $\pm$ 0.010	45 $\pm$ 3	55 $\pm$ 3
SC8	100	0.160 $\pm$ 0.010	18 $\pm$ 1	82 $\pm$ 1
	50	0.270 $\pm$ 0.010	30 $\pm$ 2	70 $\pm$ 2**
	25	0.390 $\pm$ 0.010	40 $\pm$ 3	60 $\pm$ 3*
Acarbose	100	0.220 $\pm$ 0.010	25 $\pm$ 2	75 $\pm$ 2
	50	0.320 $\pm$ 0.010	40 $\pm$ 3	60 $\pm$ 3
	25	0.460 $\pm$ 0.010	55 $\pm$ 3	45 $\pm$ 3

Values are expressed in mean $\pm$ SD, ( $n = 3$ )

Table 5 shows the  $\alpha$ -amylase inhibition activity of SC2, SC8 and Acarbose at different concentrations (100, 50, and 25  $\mu\text{g/mL}$ ). At a concentration of 100  $\mu\text{g/mL}$ , SC2 exhibits an inhibition of  $80\pm 2\%$ , while SC8 has slightly higher inhibition at  $82\pm 1\%$ . In comparison, Acarbose demonstrates lower inhibition at  $75\pm 2\%$ . This indicates that SC2 and SC8 have a more potent inhibitory effect on  $\alpha$ -amylase than Acarbose at the highest concentration tested. At lower concentrations (50  $\mu\text{g/mL}$  and 25  $\mu\text{g/mL}$ ), SC2 and SC8 continue to display higher  $\alpha$ -amylase inhibition than Acarbose. At 50  $\mu\text{g/mL}$ , SC2 has an inhibition of  $65\pm 2\%$  and SC8 exhibits an inhibition of  $70\pm 2\%$  compared to Acarbose with  $60\pm 3\%$  inhibition. Similarly, at 25  $\mu\text{g/mL}$ , SC2 and SC8 inhibit  $\alpha$ -amylase by  $55\pm 3\%$  and  $60\pm 3\%$ , respectively, while Acarbose shows a lower inhibition of  $45\pm 3\%$ .

Table 6

**IC<sub>50</sub> values for  $\alpha$ -amylase inhibition activity of compounds SC2, SC8 and Acarbose**

Compound	IC <sub>50</sub> Value ( $\mu\text{g/mL}$ )
SC2	$36.5\pm 1.5$
SC8	$45.2\pm 2.1$
Acarbose	$68.9\pm 3.2$

Values are expressed in mean $\pm$ standard deviation ( $n = 3$ )

Table 6 presents the IC<sub>50</sub> values for  $\alpha$ -amylase inhibition activity of SC2, SC8 and Acarbose. The IC<sub>50</sub> value represents the concentration of the compound required to inhibit 50 % of the enzyme activity. SC2 has the lowest IC<sub>50</sub> value of  $36.5\pm 1.5$   $\mu\text{g/mL}$ , followed by SC8 at  $45.2\pm 2.1$   $\mu\text{g/mL}$ , and Acarbose with the highest IC<sub>50</sub> value of  $68.9\pm 3.2$   $\mu\text{g/mL}$ . These results indicate that SC2 is the most potent inhibitor among the three compounds, requiring a lower concentration to achieve 50% inhibition of  $\alpha$ -amylase activity.

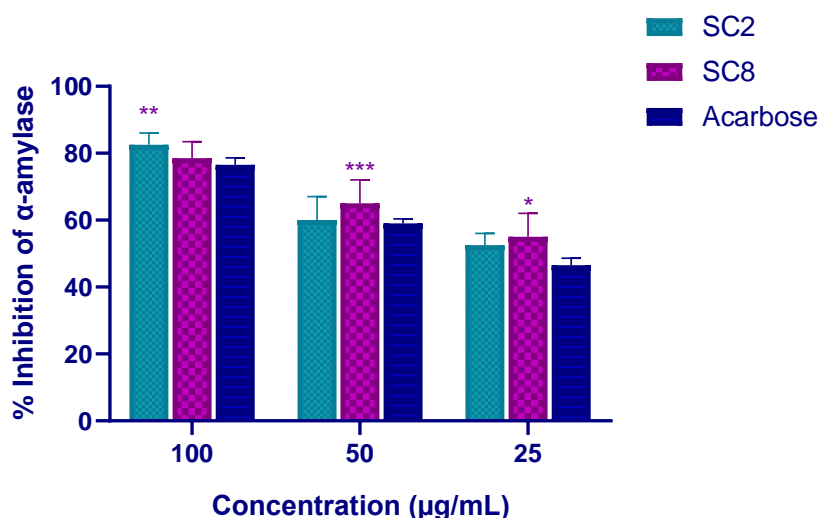


Figure 7 Graphical Representation of  $\alpha$ -amylase inhibition activity of compounds SC2, SC8 and Acarbose

Figure 7 graphically represents the  $\alpha$ -amylase inhibition activity of SC2, SC8 and Acarbose at different concentrations. The plot further illustrates that SC2 and SC8 exhibit superior inhibition compared to Acarbose across all tested concentrations. In conclusion, the results of the  $\alpha$ -amylase inhibition activity assay indicate that SC2 and SC8 are more potent inhibitors of  $\alpha$ -amylase than Acarbose at all tested concentrations. Furthermore, SC2 displays the highest potency among the three compounds, with the lowest IC<sub>50</sub> value of  $36.5\pm 1.5$   $\mu\text{g/mL}$ . These findings suggest that SC2 and SC8 hold promise as potential therapeutic agents for the inhibition of  $\alpha$ -amylase, with SC2 being the most effective. Further studies are needed to assess the in vivo efficacy and safety profile of these compounds as potential therapeutics for conditions that could benefit from  $\alpha$ -amylase inhibition, such as diabetes.

### Conclusions

In conclusion, this research article has successfully designed and analyzed a series of 1,3,4-oxadiazole derivatives as potential  $\alpha$ -amylase inhibitors. Through *in silico* ADMET analysis, Lipinski's Rule of Five and drug-likeness evaluation, the study has identified two promising candidates, SC2 and SC8, that exhibit favorable pharmacokinetic properties and drug-likeness characteristics. Molecular docking studies reveal strong binding affinities of these compounds to the target protein, human  $\alpha$ -amylase (PDB ID: 6Z8L), and provide insights into the key interactions responsible for their inhibitory activities. The *in vitro*  $\alpha$ -amylase inhibition assay demonstrates that both SC2 and SC8 exhibit more potent inhibitory activities against  $\alpha$ -amylase than the reference compound Acarbose across all tested concentrations. Notably, SC2 is the most effective inhibitor, with the lowest  $IC_{50}$  value of  $36.5 \pm 1.5 \mu\text{g/mL}$ . These findings suggest that SC2 and SC8 hold significant potential as therapeutic agents for the inhibition of  $\alpha$ -amylase and could serve as a basis for the advancement in novel therapies for diabetes. Despite these promising results, further investigations are required to confirm the *in vivo* efficacy and safety profile of SC2 and SC8 as potential therapeutic agents. Future studies should focus on evaluating the pharmacodynamic properties, toxicity and long-term effects of these compounds in animal models, followed by human clinical trials. Additionally, structure-activity relationship (SAR) studies could be conducted to optimize the molecular structures of these compounds for enhanced potency, selectivity and reduced side effects. Overall, this research article presents valuable findings that contribute to the ongoing search for novel and effective  $\alpha$ -amylase inhibitors in the treatment of diabetes and other related disorders.

### Acknowledgments

Authors would like to express their deepest gratitude to the Principal of SND College of Pharmacy, Yeola, for their unwavering support and generosity in providing all the necessary facilities to conduct the research experiments. Also, the authors are obliged to Principal and management of Mahavir Institute of Pharmacy, Nashik for providing necessary facilities.

### References

- 1 American Diabetes Association (2014). Diagnosis and classification of diabetes mellitus. *Diabetes care*, 37 Suppl 1, S81–S90. <https://doi.org/10.2337/dc14-S08>
- 2 Kaul, K., Tarr, J. M., Ahmad, S. I., Kohner, E. M., & Chibber, R. (2012). Introduction to diabetes mellitus. *Advances in experimental medicine and biology*, 771, 1–11. [https://doi.org/10.1007/978-1-4614-5441-0\\_1](https://doi.org/10.1007/978-1-4614-5441-0_1)
- 3 Alam, U., Asghar, O., Azmi, S., & Malik, R. A. (2014). General aspects of diabetes mellitus. *Handbook of clinical neurology*, 126, 211–222. <https://doi.org/10.1016/B978-0-444-53480-4.00015-1>
- 4 Bashary, R., Vyas, M., Nayak, S. K., Sutte, A., Verma, S., Narang, R., & Khatik, G. L. (2020). An Insight of Alpha-amylase Inhibitors as a Valuable Tool in the Management of Type 2 Diabetes Mellitus. *Current diabetes reviews*, 16(2), 117–136. <https://doi.org/10.2174/1573399815666190618093315>
- 5 Yakkala, P. A., Khan, I. A., Dannarm, S. R., Aboti, J., Sonti, R., Shafi, S., & Kamal, A. (2023). Multicomponent Domino Reaction for Concise Access to 2-Amino-Substituted 1,3,4 Oxadiazoles via Smiles Rearrangement. *The Journal of Organic Chemistry*, 88(17), 12216–12223. <https://doi.org/10.1021/acs.joc.3c00516>
- 6 Bukhari, A., Nadeem, H., Imran, M., & Muhammad, S. A. (2021). Novel oxadiazole derivatives as potent inhibitors of  $\alpha$ -amylase and  $\alpha$ -glucosidase enzymes: Synthesis, *in vitro* evaluation, and molecular docking studies. *Iranian journal of basic medical sciences*, 24(12), 1632–1642. <https://doi.org/10.22038/IJBMS.2021.58429.12977>
- 7 Hamdani, S. S., Khan, B. A., Ahmed, M. N., Hameed, S., Akhter, K., Ayub, K., & Mahmood, T. (2020). Synthesis, crystal structures, computational studies and  $\alpha$ -amylase inhibition of three novel 1, 3, 4-oxadiazole derivatives. *Journal of Molecular Structure*, 1200, 127085. <https://doi.org/10.1016/j.molstruc.2019.127085>
- 8 Badithapuram, V., Nukala, S. K., Thirukovela, N. S., Dasari, G., Manchal, R., & Bandari, S. (2022). Design, synthesis, and molecular docking studies of some new quinoxaline derivatives as EGFR targeting agents. *Russian Journal of Bioorganic Chemistry*, 48(3), 565–575. <https://doi.org/10.1134/S106816202203022>
- 9 Zhang, S., Luo, Y., He, L. Q., Liu, Z. J., Jiang, A. Q., Yang, Y. H., & Zhu, H. L. (2013). Synthesis, biological evaluation, and molecular docking studies of novel 1,3,4-oxadiazole derivatives possessing benzotriazole moiety as FAK inhibitors with anticancer activity. *Bioorganic & medicinal chemistry*, 21(13), 3723–3729. <https://doi.org/10.1016/j.bmc.2013.04.043>
- 10 Bitla, S., Sagurthi, S. R., Dhanavath, R., Puchakayala, M. R., Birudaraju, S., Gayatri, A. A., ... & Atcha, K. R. (2020). Design and synthesis of triazole conjugated novel 2, 5-diaryl substituted 1, 3, 4-oxadiazoles as potential antimicrobial and anti-fungal agents. *Journal of Molecular Structure*, 1220, 128705. <https://doi.org/10.1016/j.molstruc.2020.128705>



- 11 Perla, P., Seelam, N., & Bera, R. (2020). Design and synthesis of novel 1a, 3, 4-oxadiazole derivatives as cytotoxic agents: a combined experimental and docking study. *Russian Journal of Organic Chemistry*, 56, 924-934 <https://doi.org/10.1134/S1070428020050280>
- 12 Srinivasa, M. G., Paithankar, J. G., SahebBirangal, S. R., Pai, A., Pai, V., Deshpande, S. N., & Revanasiddappa, B. C. (2023). Novel hybrids of thiazolidinedione-1,3,4-oxadiazole derivatives: synthesis, molecular docking, MD simulations, ADMET study, in vitro, and in vivo anti-diabetic assessment. *RSC Advances*, 13(3), 1567–1579. <https://doi.org/10.1039/d2ra07247e>
- 13 Wang, Y., Xing, J., Xu, Y., Zhou, N., Peng, J., Xiong, Z., Liu, X., Luo, X., Luo, C., Chen, K., Zheng, M., & Jiang, H. (2015). In silico ADME/T modelling for rational drug design. *Quarterly reviews of biophysics*, 48(4), 488–515. <https://doi.org/10.1017/S0033583515000190>
- 14 Jafari, E., Mohammadi, T., Jahanian-Najafabadi, A., & Hassanzadeh, F. (2017). Synthesis and antimicrobial evaluation of some 2,5 disubstituted 1,3,4-oxadiazole derivatives. *Research in pharmaceutical sciences*, 12(4), 330–336. <https://doi.org/10.4103/1735-5362.212051>
- 15 Radia, A. J., Lalpara, J. N., Modasiya, I. J., & Dubal, G. G. (2021). Design and synthesis of novel 1, 3, 4-oxadiazole based azaspirocyclohexane catalyzed by NaI under mild condition and evaluated their antidiabetic and antibacterial activities. *Journal of Heterocyclic Chemistry*, 58(2), 612-621. <https://doi.org/10.1002/jhet.4200>
- 16 Zhou, L., Wang, P. Y., Zhou, J., Shao, W. B., Fang, H. S., Wu, Z. B., & Yang, S. (2017). Antimicrobial activities of pyridinium-tailored pyrazoles bearing 1, 3, 4-oxadiazole scaffolds. *Journal of Saudi Chemical Society*, 21(7), 852-860. <https://doi.org/10.1016/j.jscs.2017.04.005>
- 17 Li, Y., Luo, Y., Hu, Y., Zhu, D. D., Zhang, S., Liu, Z. J., Gong, H. B., & Zhu, H. L. (2012). Design, synthesis and antimicrobial activities of nitroimidazole derivatives containing 1,3,4-oxadiazole scaffold as FabH inhibitors. *Bioorganic & medicinal chemistry*, 20(14), 4316–4322. <https://doi.org/10.1016/j.bmc.2012.05.050>
- 18 Khalilullah, H., Ahsan, M. J., Hedaitullah, M., Khan, S., & Ahmed, B. (2012). 1,3,4-oxadiazole: a biologically active scaffold. *Mini reviews in medicinal chemistry*, 12(8), 789–801. <https://doi.org/10.2174/138955712801264800>
- 19 Acar Çevik, U., Celik, I., Paşayeva, L., Fatullayev, H., Bostancı, H. E., Özkay, Y., & Kaplancıklı, Z. A. (2023). New benzimidazole-oxadiazole derivatives: Synthesis,  $\alpha$ -glucosidase,  $\alpha$ -amylase activity, and molecular modeling studies as potential antidiabetic agents. *Archiv der Pharmazie*, 356(5), e2200663. <https://doi.org/10.1002/ardp.202200663>
- 20 Khan, B. A., Hamdani, S. S., Ahmed, M. N., Hameed, S., Ashfaq, M., Shawky, A. M., Ibrahim, M. A. A., & Sidhom, P. A. (2022). Synthesis, X-ray diffraction analysis, quantum chemical studies and  $\alpha$ -amylase inhibition of probenecid derived S-alkylphthalimide-oxadiazole-benzenesulfonamide hybrids. *Journal of enzyme inhibition and medicinal chemistry*, 37(1), 1464–1478. <https://doi.org/10.1080/14756366.2022.2078969>
- 21 Lima, L. R., Bastos, R. S., Ferreira, E. F. B., Leão, R. P., Araújo, P. H. F., Pita, S. S. D. R., De Freitas, H. F., Espejo-Román, J. M., Dos Santos, E. L. V. S., Ramos, R. D. S., Macêdo, W. J. C., & Santos, C. B. R. (2022). Identification of Potential New *Aedes aegypti* Juvenile Hormone Inhibitors from N-Acyl Piperidine Derivatives: A Bioinformatics Approach. *International journal of molecular sciences*, 23(17), 9927. <https://doi.org/10.3390/ijms23179927>
- 22 Al-Wahaibi, L. H., Mohamed, A. A. B., Tawfik, S. S., Hassan, H. M., & El-Emam, A. A. (2021). 1,3,4-Oxadiazole N-Mannich Bases: Synthesis, Antimicrobial, and Anti-Proliferative Activities. *Molecules (Basel, Switzerland)*, 26(8), 2110. <https://doi.org/10.3390/molecules26082110>
- 23 SarveAhrabi, Y., Ahrabi, N. Z., & Souldozi, A. (2021). Synthesis and antimicrobial evaluation of new series of 1,3,4-oxadiazole containing cinnamic acid derivatives. *Avicenna Journal of Clinical Microbiology and Infection*, 8(1), 11–16. <https://doi.org/10.34172/ajcmi.2021.03>
- 24 Glomb, T., & Świątek, P. (2021). Antimicrobial activity of 1,3,4-oxadiazole derivatives. *International journal of molecular sciences*, 22(13), 6979. <https://doi.org/10.3390/ijms22136979>
- 25 Bala, S., Kamboj, S., Kajal, A., Saini, V., & Prasad, D. N. (2014). 1,3,4-oxadiazole derivatives: synthesis, characterization, antimicrobial potential, and computational studies. *BioMed research international*, 2014, 172791. <https://doi.org/10.1155/2014/172791>
- 26 Karande, N.A., Rathi, L.G., Kamble, K.S. et al. (2023) Synthesis, Anti-Inflammatory Activity and Molecular Docking Studies of New 1,2,4-Triazolo[3,4-b][1,3,4]Thiadiazine Derivatives. *Pharm Chem J*, 57, 234–242. <https://doi.org/10.1007/s11094-023-02873-6>
- 27 Bendale, A. R., Bhatt, R., Nagar, A., Jadhav, A. G., & Vidyasagar, G. (2011). Schiff base synthesis by unconventional route: An innovative green approach. *Der Pharma Chemica*, 3(2), 34–38.

#### Information about authors\*

**Chavan, Shivani U.** (*corresponding author*) — Research Student, Department of Pharmaceutical Chemistry, S.N.D. College of Pharmacy, Babhulgaon, 423401, Nashik, India; e-mail: [shivanichavan26@gmail.com](mailto:shivanichavan26@gmail.com), <https://orcid.org/0009-0009-8805-8699>

**Waghmare, Sonali A.** — Assistant Professor, Department of Pharmaceutical Chemistry, S.N.D. College of Pharmacy, Babhulgaon, 423401, Nashik, India; e-mail: [waghmaresonali877@gmail.com](mailto:waghmaresonali877@gmail.com)

**Bodke, Shraddha S.** — Research Student, Department of Pharmaceutical Chemistry, Mahavir Institute of Pharmacy, Varvandi, 422004, Nashik, India; e-mail: [shraddhabodke32@gmail.com](mailto:shraddhabodke32@gmail.com), <https://orcid.org/0000-0002-0765-7553>

**Bendale, Atul R.** — Professor, Department of Pharmaceutical Chemistry, Mahavir Institute of Pharmacy, Varvandi, 422004, Nashik, India; e-mail: [atulbendale123@gmail.com](mailto:atulbendale123@gmail.com), <https://orcid.org/0000-0002-3219-0377>

---

\*The author's name is presented in the order: *Last Name, First and Middle Names*